PROCEEDINGS OF THE TECHNICAL UNIVERSITY OF SOFIA, ISSN: 2738-8549, 2738-8530 VOL. 76, NO. 3, YEAR 2026

A wind tunnel study of wingtip devices for small unmanned airplanes

Wajdi Jaffela, Shayma Kacem, Vladimir Serbezov, Michael Todorov

***Abstract*—The paper presents the results of a student project to study the aerodynamic characteristics of two common types of wingtip devices in the wind tunnel of the National Center for Mechatronics and Clean Technologies (NCMCT). The wingtip devices examined were canted winglet and wingtip fence. As a baseline configuration the wing without wingtip device was used. The tests were conducted at airspeeds of 12 m/s corresponding to Reynolds number of approximately 10000. The results correspond well to the theoretical expectations and prove the advantage of canted winglet over the other configurations. The results can be used in the future for the purpose of adjusting and validating CFD models of wingtip devices for low-speed small unmanned airplanes.**

1

***Keywords*—Aerodynamic characteristics, UAV, Wind tunnels, Winglets**

I. Introduction

Wingtip devices like various types of winglets, wingfences, etc. are popular means for minimizing the induced drag of manned and unmanned aircraft without increasing the wingspan. Most of the fundamental research in the area was stimulated by the petrol crisis in the 1970-x [1, 2] and was implemented in the passenger aircraft of the late 1980-x like the Airbus 320 family. Since then different types of wingtip devices are used for all types of fixed wing aircraft. Comprehensive overviews of the subject are presented in [3, 4]. Publications [3, 4] can be used also as design guides for wingtip devices.

Even though the subject is well studied theoretically, the ongoing relevance of experimental studies of wingtip devices for small-unmanned aircraft is caused by the fact that they operate at very low Reynolds numbers where the theoretical and computational models can not deliver satisfactory results accuracy. Examples of present days experimental studies on the aerodynamic characteristics of wingtip devices are the works [5, 6].

The aim of the present work is not so much to evaluate the aerodynamic characteristics of particular wingtip devices, but to establish and verify a methodology for such experimental evaluation in the wind tunnel of the NCMCT. For this purpose two typical wingtip devices, namely a classic Airbus type wingfence (Fig. 1b) and a winglet (Fig. 1c) were produced and tested in the wind tunnel and their aerodynamic characteristics were compared with those of the wing without special wingtip.

II. Wingtip devices design and fabrication

As a base wing, a rectangular wing with span of 400 mm, chord 130 mm and NACA 4412 airfoil is used (Fig. 1a). The wing was produced as a part of the preceding Master's project of Kamergy [7].

Both wingtip devices are designed in Solidworks, using the methodology described in [4] and then were 3D printed to be easily installed and then removed from the wingtip.

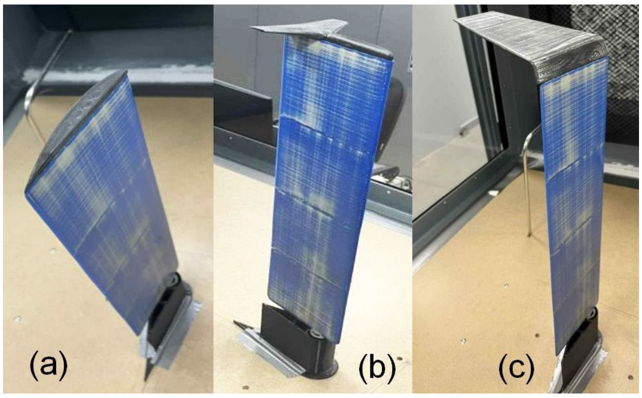

Fig. 1. Tested configurations installed in the wind tunnel: (a) No wingtip device, (b) wingfance, (c) winglet.

The wingfence uses NACA 0010 airfoil. Its main dimensions are shown on Fig. 2.

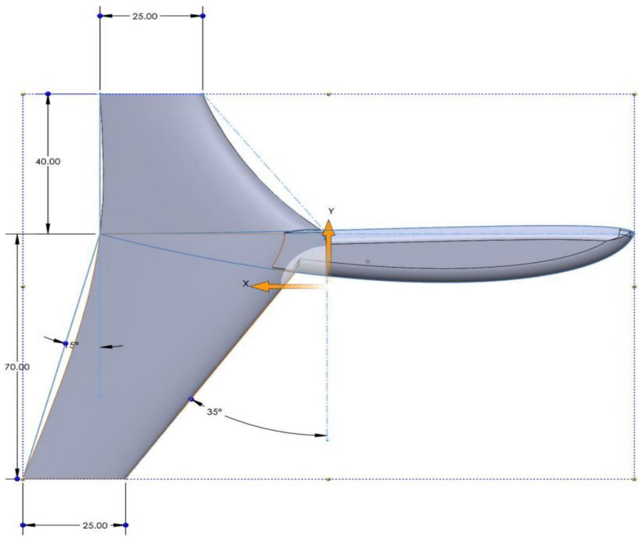

Fig. 2. Wingfence main geometric parameters.

Received: 01.07.2026
Published: 27.07.2026
https://doi.org/10.47978/TUS.2026.76.03.006

Wajdi Jaffela is with the EPI Polytechnique, Belt Road, Sahloul, Sousse 4021 Tunisia (jaffelawajdi@gmail.com)

Chaima Kacem is with the EPI Polytechnique, Belt Road, Sahloul, Sousse 4021 Tunisia (kacemshayma28@gmail.com)

Vladimir Serbezov is with the Technical University of Sofia, Sofia, 1000, 8 Kl. Ohridski Blvd, Bulgaria (vserbezov@tu-sofia.com)

Michael Todorov is with the Technical University of Sofia, Sofia, 1000, 8 Kl. Ohridski Blvd, Bulgaria (michael.todorov@tu-sofia.com)

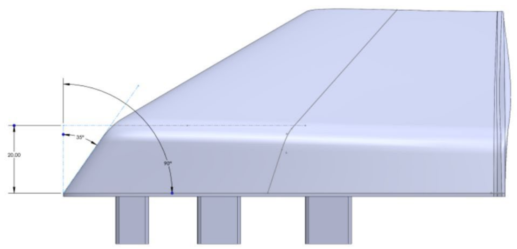

Fig. 3. Bottom view of the winglet.

The winglet is designed in a similar manner, using NACA 4412 airfoil with leading edge sweep angle of 35°, cant angle of 25° from the vertical and height of 100 mm. On Fig. 3 a bottom view of the winglet is presented with winglet-wing attachment teeth (same as for the wingfence) clearly observable.

III. WIND TUNNEL TEST SETUP

A principal scheme of the NCMCT wind tunnel with the test setup is shown on Fig. 4. The wind tunnel is an open loop type tunnel with closed test section. The test section is 800 mm high, 100 mm wide and 140 mm long. The wind tunnel is capable to operate with airspeed from 3 m/s to around 21 m/s.

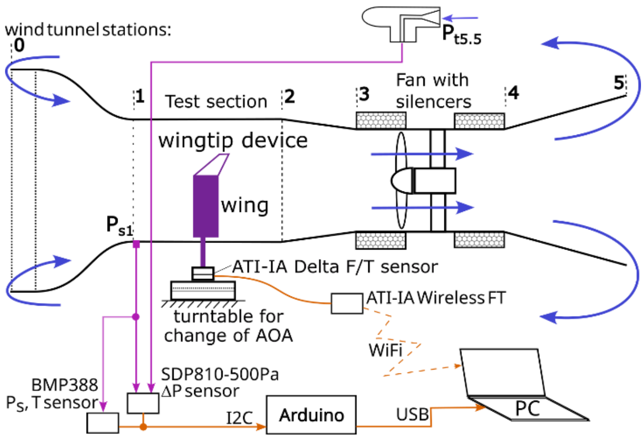

Fig. 4. Wind tunnel and experimental setup.

A. *Air data measurement*

The air data measurement system of the wind tunnel consists of two sensors connected through an Arduino board to the data-collecting computer. The first sensor is an absolute pressure sensor BMP388, measuring the static pressure at the entrance of the wind tunnel test section (designated P_{s1}). This sensor measures also the air temperature T_{s1}, thus allowing the calculation of the air density. The second sensor is a differential pressure sensor SDP810-500Pa. It measures the difference between the total pressure in the space around the wind tunnel ($P_{t5.5}$) and P_{s1}. The airspeed at the test section entrance is calculated based on the differential pressure and an experimentally obtained correction factor.

The Arduino board collects the data from the pressure sensors and sends it to the computer (PC) with a rate of about five samples per second.

B. *Wing installation and force measurement*

The wing is mounted on a steel tube that passes through the floor panel of the test section. The tube is connected to the force/torque sensor via a fitting. The sensor is fixed on a turn table that allows precise manual adjustment of the angle of attack (AOA) of the wing.

The aerodynamic forces and moments acting on the tested wing are measured by a six-component force/torque sensor ATI-IA Delta. The sensor is connected to an ATI-IA WirelessFT measurement system. The system sends the measured data to the data-collecting PC via Wi-Fi with a rate of 100 samples per second.

IV. METHODOLOGY

A. *General description of the test sequence*

The tests of every wing configuration were carried out at constant power setting of the wind tunnel fan motor, providing almost the same air velocity for all angles of attack. Figure 5 shows the test sequence of one of the wingtip configurations. The angle of attack was changed manually by one of the experimenters at steps of at least 10 seconds. After each change the experimenter manually indicated it by producing a small shock on the turntable basement, that was recorded by the force sensor. These shocks can be observed on Fig. 5 as green vertical lines. The executed AOA sequence was -10, -5, 0, 5, 10, 12, 14, 16, 18, 20, 22 degrees. The AOA data was entered manually in the PC after analyzing the test sequence of every wingtip configuration.

Before further processing the data is smoothed and the parts of the record with transitions in the air velocity or angle of attack are excluded.

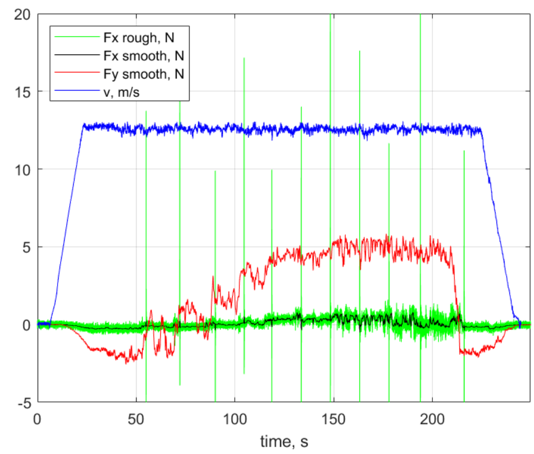

Fig. 5. Typical wind tunnel test sequence.

B. *Data processing*

After acquiring the test data it is processed in Matlab in the following steps:

1. Calculating the air density

For all recorded data points the air density is calculated based on the static Pressure and temperature in aerodynamic station 1 of the wind tunnel (see Fig. 4):

$$\rho = \frac{P_{S1}}{R.T_{S1}} \tag{1}$$

where $R = 287\ J/(kg.K)$ is the dry air gas constant.

2. Calculating the air velocity

The velocity is calculated with regard to the points in which the pressures are measured:

$$v = \sqrt{\frac{2k.(P_{t5.5} - P_{s1})}{\rho}} \quad (2)$$

where k is an experimentally determined coefficient accounting for the total pressure loss between the wind tunnel aerodynamic stations 5.5 and 1 (see Fig. 4).

3. Calculating the Reynolds number

$$Re = \frac{\rho.v.c}{\mu} \quad (3)$$

where $c=0.13\ m$ is the wing chord. The dynamic viscosity of the air μ is calculated using the Sutherland's Law:

$$\mu = \mu_0.\left(\frac{T_{S1}}{T_0}\right)^{3/2}.\frac{T_0+S_\mu}{T_{S1}+S_\mu} \quad (4)$$

where $\mu_0 = 1.716.10^{-5}\ N.s/m^2$, $T_0 = 273K$, $S_\mu = 111K$ is the Sutherland's constant for air.

4. Lift and drag coefficients in the wing (the F/T sensor) coordinate system

$$c_L = \frac{2.F_y}{\rho.v^2.S} \quad (5)$$

where c_L is the lift coefficient, F_y is the force measured by the F/T sensor in the lateral direction and $S = 0.052\ m^2$ is the wing area.

$$c_D = \frac{2.F_x}{\rho.v^2.S} \quad (6)$$

where c_D is the drag coefficient, F_x is the force measured by the F/T sensor in the axial direction.

5. Lift and drag coefficients in the velocity coordinate system (aerodynamic lift and drag coefficients)

$$c_{La} = c_L.\cos\alpha - c_D \sin\alpha \quad (7)$$
$$c_{Da} = c_L.\sin\alpha - c_D \cos\alpha \quad (8)$$

where c_{La} and c_{Da} are respectively the lift and drag coefficients in the velocity coordinate system and α is the angle of attack of the wing.

6. Mean values calculation

Mean values of the aerodynamic lift and drag coefficients are calculated for each angle of attack.

After all these steps, the results are plotted for further analysis.

V. RESULTS

The tests are carried out at air velocities of little over 12 m/s, corresponding to Reynolds numbers of around 100000.

A combined graphic of the aerodynamic lift coefficient in function of the angle of attack for the three wingtip configurations is shown in Fig. 6.

The overall appearance of the graphs corresponds to their theoretical shape, which is an indicator of the methodology's validity. The maximum value of the lift coefficient, approximately 1.0 – 1.2, is significantly lower, and the critical angle of attack of 16 degrees is greater than those for the NACA 4412 airfoil at Re = 10e4 (1.5 and 14 degrees, respectively), as taken from the web-based database airfoiltools.com. This is explained by the low Reynolds number and the low aspect ratio (3.08) of the tested wing.

It is evident that the winglet configuration has significantly higher lift coefficient at moderate to high angles of attack (5° - 15°). Wing fence configuration do not demonstrate any advantage.

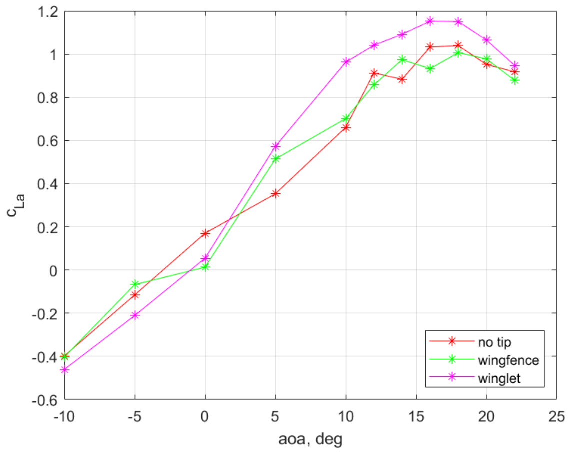

Fig. 6. Aerodynamic lift coefficient in function of angle of attack.

Figure 7 shows the wing aerodynamic polar. Again, the polars fully correspond to the theoretical shapes. The winglet configuration demonstrates higher drag at low lift conditions because of the higher wet area and so higher friction drag. At high lift because of the lower induced drag, the total drag is significantly smaller. It can be said that the wing with the wingfence performs between the clear wing and the wing with winglet configurations.

The clear wing and the wingfence show some instability of the measurement results. This shows a need for improvement of the test methodology.

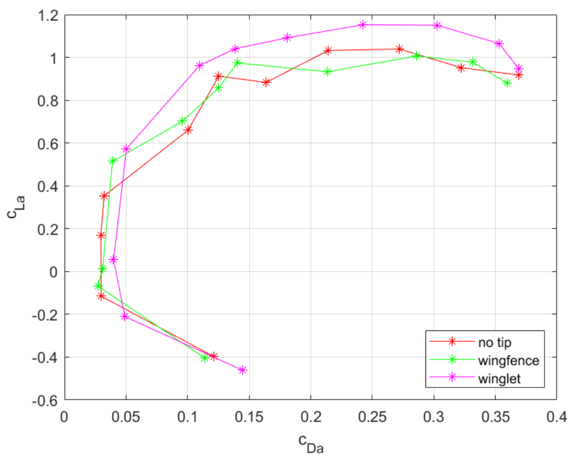

Fig. 7. Wing polar.

Interesting conclusions may be drawn from the lift to drag ratio (L/D) over lift coefficient graphic shown on Fig. 8. It is evident that at aerodynamic lift coefficients from 0.3 to almost 0.6 the wingfence has clear advantage over the other two configurations in terms of L/D (reaching 13). It should be pointed, as evident from Fig. 7, that at point of highest L/D the wingfence lift coefficient is a little bit lower than that of the winglet, but the effect comes from the much lower wingfence drag coefficient. As far as these are typical values of the lift coefficient for cruise flight, it turns that a smaller wingfence may be the preferable configuration for certain class of aircraft, rather than a larger area winglet.

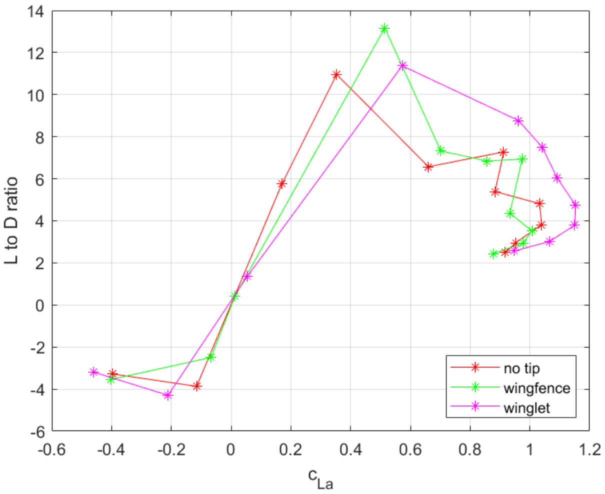

Fig. 8. Lift to drag ratio in function of aerodynamic lift coefficient.

VI. Conclusion

The conducted aerodynamic experiments of three configurations of the wingtip of the tested wing generally met the expectations. The tested winglet has superior performance at high angles of attack, booth in terms of higher lift coefficient and better L/D ratio. At the same time the wingfence showed better performance and the highest L/D ratio at moderate angles of attack. These results are good illustration of the complexity of the wing optimization problem. They also validate the performed test methodology.

The obtained curves show some undesirable deviations from the smooth shape. In future experiments this could be overcome by reducing the angle of attack step and increasing the duration of each step in order to increasing the number of data points available for ensemble averaging.

Further work may include also testing of more variants of wingtip devices and parametrization of the results. The presented wind tunnel testing methodology has very good potential for students training and yang researcher work.

Acknowledgment

This research was funded by the scientific-research project № 253CH0001-04 "Development of infrastructure and environment for aerospace education and research at TU-Sofia /INSATUS/" by the contract with "Research and development sector at TU-Sofia".

References

[1] Whitcomb, R. T. (1976). A design approach and selected wind tunnel results at high subsonic speeds for wing-tip mounted winglets (No. L-10908).

[2] Heyson, H. H., Riebe, G. D., & Fulton, C. L. (1977). Theoretical parametric study of the relative advantages of winglets and wing-tip extensions (No. NASA-TM-X-74003).

[3] Makgantai, B., Subaschandar, N., & Jamisola, R. S. (2021). A review on wingtip devices for reducing induced drag on fixed-wing drones. [Online] https://repository.biust.ac.bw/bitstream/handle/123456789/403/Makgantai_Journal%20of%20Xi'an%20University%20of%20Architecture%20&%20Technology_2021.pdf?sequence=3&isAllowed=y

[4] Rajendran, S. (2012). Design of Parametric Winglets and Wing tip devices: A conceptual design approach. [Online] https://www.diva-portal.org/smash/get/diva2:547954/FULLTEXT01.pdf

[5] Penchev, S., & Panayotov, H. (2025). A Wind Tunnel Study of the Aerodynamic Characteristics of Wings with Arc-Shaped Wingtips. Engineering Proceedings, 100(1), 28.

[6] Nikolaou, E., Kilimtzidis, S., & Kostopoulos, V. (2025). Winglet Design for Aerodynamic and Performance Optimization of UAVs via Surrogate Modeling. Aerospace, 12(1), 36.

[7] Kamergi, Y., (2025). Experimental study of airfoils in a wind tunnel. [Unpublished master's thesis]. Department of Aeronautics, Technical University of Sofia.